

TRMM Available Products

[As of November 15, 2022.]

Standard Products

Processing Level	Satellite / Instrument	Product [Product Identifier]	Key Parameters	File coverage	Available Latest Product Version (Caveats)
1	TRMM/PR	PR L1B [PU1]	Received Power	TRMM orbit (Torbit*)	Ver. 07 (See: page 2)
	TRMM/TMI	TMI L1B [TMI]	Brightness Temperature (Tb)	Torbit	Ver. 07 (See: page 3)
	TRMM/TMI	TMI L1C [TMI]	Inter-Calibrated Brightness Temperature (Tb)	Torbit	Ver. 07 (See: page 3)
	TRMM/VIRS	VIRS L1B [V1B]	Radiance	Torbit	Ver. 07 (To be prepared)
2	TRMM/PR	PR L2 [PU2]	Reflectivities, 3D Precipitation	Torbit	Ver. 07 (See: page 4)
		SLH-PR L2 [LHP]	Spectral latent heating	Torbit	Ver. 07 (See: page 6)
	TRMM/TMI/GPROF	TMI L2 [TL2]	Precipitation, Total Precipitable Water	Torbit	Ver. 07 (See: page 11)
	TRMM/PR-TMI /COMB	PR-TMI Comb L2 [TC2]	PR-TMI retrieval 3D Precipitation	Torbit	Ver. 07 (See: page 14)
3	TRMM/PR	PR L3 Daily (TEXT) [P3D]	Precipitation	0.1°x 0.1° Daily	Ver. 07 (See: page 4)
		PR L3 Daily(HDF5) [P3Q]	Precipitation	0.25° x 0.25° Daily	Ver. 07 (See: page 4)
		PR L3 Monthly [P3M]	Precipitation	0.25° x 0.25° Monthly	Ver. 07 (See: page 4)
		SLH-PR L3 Gridded orbit [LHG]	Spectral latent heating	0.5°x 0.5° Gorbit	Ver. 07 (See: page 6)
		SLH-PR L3 Monthly [LHM]	Spectral latent heating	0.5°x 0.5° Monthly	Ver. 07 (See: page 6)
	TRMM/TMI/GPROF	TMI L3 Monthly [TL3]	Precipitation	0.25° x 0.25° Monthly	Ver. 07 (See: page 11)
	TRMM/PR-TMI /COMB	PR-TMI Comb L3 [TC3]	Precipitation	0.25° x 0.25° Monthly	Ver. 07 (See: page 14)
		PR-TMI CSH L3 [CSH]	Gridded Orbital Convective Stratiform Heating	0.25° x 0.25° Gorbit	Ver. 07 (See: page 14)
PR-TMI CSH L3 [CSF]		Monthly Convective Stratiform Heating	0.25° x 0.25° Monthly	Ver. 07 (See: page 14)	

* Torbit is the TRMM orbit calculated from the southern most point back to the southern most point TRMM Product is available from the below site.
<https://gportal.jaxa.jp/gpr/>



May 17, 2022

Release Notes for the PR Version 9/GPM PR Version 07A

Level 1 products

<Major changes in the PR Level1 products from Version 8 /V06A to Version 9/V07A>

1. The format of V07A products has been changed from V05C (for example, adopting “FS”, instead of “NS”) as described in the format description. The format of the TRMM/PR is consistent of that of the GPM/DPR (in particular, the KuPR). Note that a new variable of “binMirrorImage” is set to missing value for the TRMM/PR.

Format description:

https://www.eorc.jaxa.jp/GPM/doc/product/format/en/02.GPM_DPR_L1_Product_Format_Documentation_V7_E.pdf

2. Geolocation toolkit has been updated. The following variables are added and there is no change in the existing values for the geolocation (e.g. longitude, latitude).
 - navigation/scHeadingGround
 - navigation/scHeadingOrbital
 - sunData Group
 - sunLocalTime
3. Minor bugs have been fixed. “FractionalGranuleNumber” was corrected for the processing of month boundaries. “SCorientation” was corrected for the orbits with no science data.

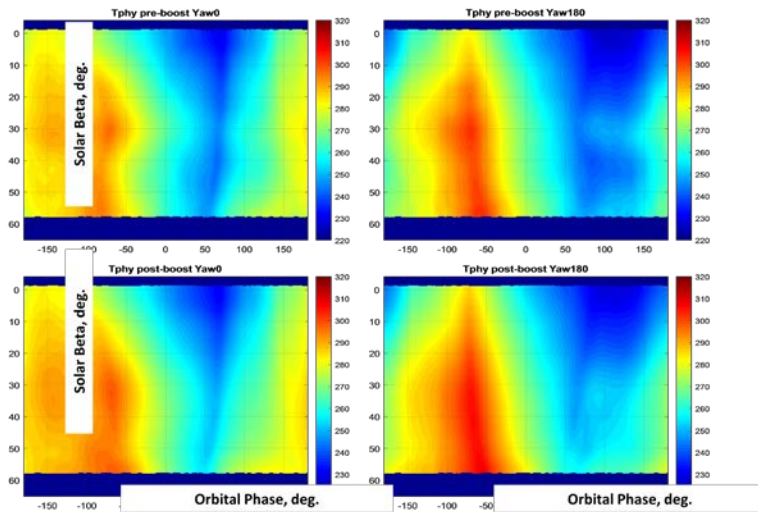
RELEASE NOTES OF GPM VERSION 07 GMI/TMI 1B/BASE

The PPS V07 GMI 1B/BASE have no calibration changes from V05 GMI 1B/BASE. However, a module is implemented to perform calibrations under conditions of missing all cold counts or all hot counts by utilizing the noise diode counts.

The PPS V07 TMI 1B/BASE applied a new Tb correction developed by UCF based on main reflector physical temperatures. The maximum Tb change is around 0.5K.

$$T_{bi} = \frac{T_{apcv8i} - T_{phyi} * \epsilon_i}{1 - \epsilon_i} \quad (2)$$

Reflector Physical Temperatures, Tphy, is functions of solar-beta-ang & orbit-phase.
Final Tphy Tables:



- Rows = Solar beta angle in deg. [-4 to 65 deg.(yaw0) and 4 to -65 deg.(yaw180) in 0.25 deg. step] > 277 rows
- Columns = Phase from orbit midnight in deg. [-180 to 180 deg. in 1 deg. step] > 361 columns
- For yaw=180, beta was reversed (i.e., beta=-1*beta;)



May 7, 2022

Release Notes for the PR Version 9/GPM PR Version 07A Level 2 and Level 3 products

<Major changes in the PR Level2 products from Version 8 /V06A to Version 9/V07A>

1. The format of V07A products has been changed from V06A (for example, adopting “FS”, instead of “NS”) as described in the ATBD. The format of the TRMM/PR is consistent of that of the GPM/DPR (in particular, the KuPR).
2. PR data are processed by essentially the similar algorithm that is used to process the DPR/KuPR data. However, algorithm differences in a scattering database appeared in V07A. In V06A, the scattering table of KuPR is used for PR by neglecting the difference of frequency (13.6 GHz for KuPR and 13.8 GHz for PR). In V07A, we implemented the scattering table calculated for 13.8GHz in the TRMM/PR algorithm. Preliminary analyses showed a histogram of PR precipitation estimates became closer to that of KuPR precipitation estimates.
3. There are several improvements associated with the DPR V07A algorithm developments. In V07A, the improved sidelobe clutter removal routine was implemented for the single frequency (KuPR, KaPR, and PR) L2 algorithms based on the results of Kanemaru et al. (2020, 2021). In addition, a new 3-D precipitation judgment method is implemented to improve the detectability of precipitation signals. This method uses signals not only in the vertical direction but also the in cross-track and along-track directions. See the ATBD for full descriptions.

Caveat:

1. PR’s rain estimates over land have significantly (about 15%) increased in V07A from V06A because of considering a soil moisture effect. Please see Seto et al. (2022) for the soil moisture effect. The PR estimates over ocean have decreased slightly.

Reference:

GPM/DPR Level-2 Algorithm Theoretical Basis Document, available from

https://arthurhou.pps.eosdis.nasa.gov/Documents/ATBD_DPR_V07A.pdf

https://arthurhou.pps.eosdis.nasa.gov/Documents/ATBD_DPR_L3_V7.pdf

Kanemaru, K., T. Iguchi, T. Masaki, and T. Kubota, 2020: Estimates of Spaceborne Precipitation Radar Pulsewidth and Beamwidth Using Sea Surface Echo Data, *IEEE Trans. Geosci. Remote Sens.*, pp.1-13, <https://doi.org/10.1109/TGRS.2019.2963090>.



May 7, 2022

Kanemaru, K., H. Hanado, K. Nakagawa, 2021: Improvement of the clutter removal method for the spaceborne precipitation radars, IGARSS2021, <https://doi.org/10.1109/IGARSS47720.2021.9554974>

Seto, S., T. Iguchi, and R. Meneghini, 2022: Correction of path integrated attenuation estimates considering the soil moisture effect for the GPM Dual-frequency Precipitation Radar, *J. Atmos. Oceanic Technol.*, <https://doi.org/10.1175/JTECH-D-21-0111.1>

For the GPM SLH V07, the LUTs for great mountain ranges in the tropical precipitation regime ($\text{rainTypeSLH} > 200$) is newly developed. The areas of the great mountain ranges in the tropical precipitation regime are shown in Figure 1. The separation among the tropics, the great mountain ranges in the tropical precipitation regime, and midlatitudes should be done referring to the rainTypeSLH values stored in the orbital data, and described in Table 1. Note only latent heating is retrieved for great mountain ranges in the tropical precipitation regime in the GPM SLH V07. TRMM SLH V07 algorithm is the same as the GPM SLH V07 algorithm.

The LUT for mid and higher latitudes was newly developed in the GPM SLH V05. In the TRMM/GPM SLH V06A, the same LUT for mid and higher latitudes is applied and LUT for tropics is the same as TRMM SLH V7A. Some recommendations to users of orbital data are listed below, for TRMM/GPM SLH V06A retrieved as tropical precipitation or those as mid latitude precipitation.

Although the SLH algorithm and Tables are the same as GPM SLH V05 for mid-latitude and TRMM SLH V7A for tropics, respectively, because of the change in input PR/KuPR Level 2 data (2APR/2AKu), TRMM/GPM SLH V06A products differ from TRMM SLH V7A and GPM SLH V05 products, respectively.

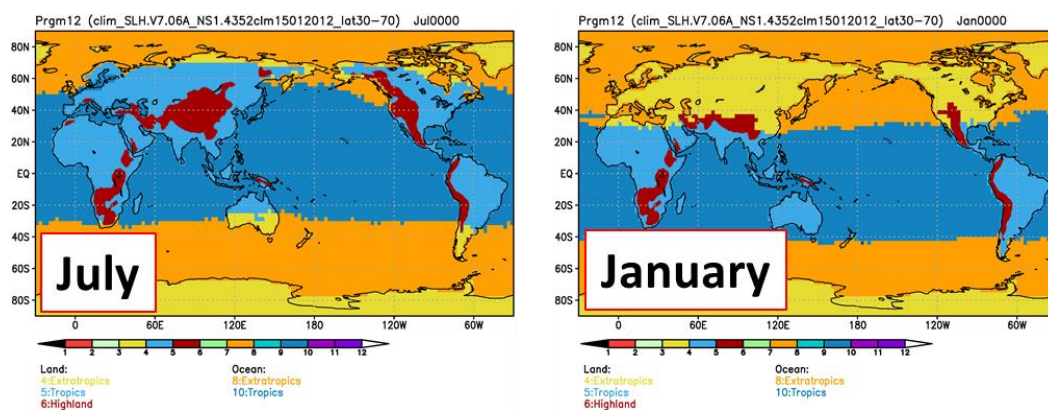


Figure 1 Distribution of the areas (6: Highland) which the LUTs for great mountain ranges in the tropical precipitation regime are applied with the areas (5: Tropics over Land and 10: Tropics over Ocean) where the LUTs for tropics are applied and the areas (4: Extratropics over Land and 8: Extratropics over Ocean) where the LUTs for mid and higher latitudes are applied for July (left) and January (right).

Table 1. Description for rainTypeSLH

(a) Tropics and subtropics	(b) Mid and higher latitudes	(c) Great mountain ranges in the tropical precipitation regime
0: No precipitation	100: No precipitation	200: No precipitation
11: Convective	111: Convective	211: Convective over high-elevation areas 212: Convective over low-elevation areas
21: Shallow stratiform	121: Shallow stratiform	221: Shallow stratiform over high-elevation areas 222: Shallow stratiform over low-elevation areas
31: Deep stratiform 32: Deep stratiform, DI (Intermediary)	131: Deep stratiform, DD, Pmax aloft 132: Deep stratiform, DD, Pmax NS 133: Deep stratiform, DI, Pmax aloft 134: Deep stratiform, DI, Pmax NS 135: Deep stratiform, subzero, Pmax aloft 136: Deep stratiform, subzero, Pmax NS	231: Deep stratiform, DD, Pmax aloft 232: Deep stratiform, DD, Pmax NS 233: Deep stratiform, DI, Pmax aloft 234: Deep stratiform, DI, Pmax NS 235: Deep stratiform, subzero, Pmax aloft 236: Deep stratiform, subzero, Pmax NS
61: Other, Applying table for rainTypeSLH=21	160: Other	261: Other, Applying table for rainTypeSLH=221 262: Other, Applying table for rainTypeSLH=222 263: Other, Applying table for rainTypeSLH=231 264: Other, Applying table for rainTypeSLH=232 265: Other, Applying table for rainTypeSLH=233 266: Other, Applying table for rainTypeSLH=234 267: Other, Applying table for rainTypeSLH=235 268: Other, Applying table for rainTypeSLH=236
Mask		
900: Areas with low melting levels including some mountains except for of great mountain ranges in the tropical precipitation regime		
910: Suspicious extreme		
920: No precipitation in SLH (precipRate < 0.2 mm/h (0.3 mm/h for tropics) or precipitation depth < 500m) but precipitation exists in 2Aku		

DI: Downward Increasing, DD: Downward Decreasing, NS: Near Surface

It was found that the change of the input KuPR level 2 data from V05 to V06 increased the bias between the KuPR near-surface precipitation and vertically integrated latent heating of SLH V06A. Moreover, some unnatural heating profiles were found associated with precipitation in tropical cyclones. To fix these problems, we revise the algorithm and release the SLH V06B product. Note that the SLH V06B product is available for GPM era since February 2014.

(i) No precipitation or Masked out pixels (rainTypeSLH=0, 100, 200, 300, 900, 910, or 920)

SLH values are not estimated (missing) for raintypeSLH=900 or 910.

SLH values are not estimated (0) for raintypeSLH=0, 100, 200, 300, 920.

(ii) Release note for tropical algorithm ($0 \leq \text{rainTypeSLH} < 100$)

Analysis showed consistency among GPM SLH V04, V05, V06 and TRMM SLH V7A, V07 estimates over the coverage of TRMM/PR during a GPM and TRMM overlapping

observation period (April-June 2014). Note that:

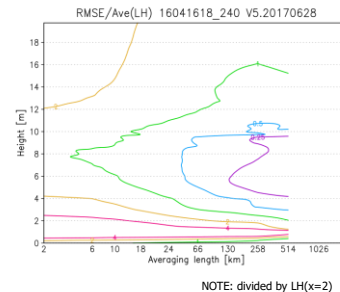
0. Vertical levels are 80 levels.
1. In the V06B SLH, there was a shallow stratiform type (`rainTypeSLH=21`). In V07 SLH this type is no longer used. Heating in all shallow pixels with their precipitation top heights (threshold 0.3mm/hr) lower than the melting level is estimated as convective type (`rainTypeSLH=11`).
2. Differences of sampling between TRMM/PR and GPM/KuPR affect SLH estimates. The greater global coverage of the GPM Core Observatory (65°N/S) compared to the TRMM coverage (35°N/S) decreases sampling of GPM/DPR over the coverage of TRMM/PR, especially at around the satellite inclination latitudes of 35°N/S, affecting SLH estimates there.
3. Retrieval for tropical cyclones and high mountains/winter mid-latitudes pixels will be developed.
4. For tropical latent heating provided in 80 levels, users are recommended to smooth the profile vertical for a few levels to avoid the spurious peak at around 0degC level.
5. The tropical algorithm is sometimes applied at high latitudes in summer. In such cases, pixels to which the tropical algorithm are applied and those to which the mid-latitude algorithm are applied are distributed disorderly. This problem will be fixed in future version.

(iii) Release Note for Mid-latitude algorithm ($100 \leq \text{rainTypeSLH} < 200$)

- A. In look up table ranges where sampling numbers did not satisfy the criteria, values are discarded or extrapolated from nearest neighbor bins, depending on the precipitation type. Sampling number criterion is basically 30, but 60 is chosen for deep stratiform LUT with precipitation maximum at the near surface level. Corresponding range for the convective LUT is $\text{PTH} > 11\text{km}$. Note that in case that a latent heating profile at the candidate bin used for extrapolation has cooling around the middle (or 0.35-0.45) of relative altitudes, for deep stratiform LUT with precipitation maximum at the near surface level, values at the bin are not used for extrapolation and those at its next bin are utilized.
- B. Recommendation for horizontal averaging at the utilization of pixel products calculated with the mid-latitude algorithm for SLP or SLG.

B1. Eddy flux convergence in Q1R and Q2 are estimated assuming that the size of “large-scale grids” is 100kmx100km. Therefore, it is recommended to average horizontally in this spatial scale to utilize Q1R or Q2.

B2. Horizontal averaging of about 50km x 50km, or 100 pixels with GPM DPR sampling, is recommended, in order to reduce root mean square errors (RMSE) calculated between estimated LH from LFM-simulated precipitation, to less than a half of the mean value at the LH peak height of ~5.5km (for Case 1).



C. CorrectionFactorMidlatType is introduced in the SLH V06B algorithm to consider LH associated with small hydrometeors condensed outside of the precipitating area, transported some distance into the precipitating area, and precipitate. However, the application of this factor in the L2 product is inconsistent in terms of pixel-by-pixel estimation. In the SLH V07 algorithm, this factor is not applied to SLP and SLG products but applied to SLM products. The specific value of the correctionFactorMidlatType is stored in the AlgorithmRuntimeInfo in the L2 product and correctionFactorMidlatType in the L3 product.

(v) Release Note for L3 (gridded; SLG and Monthly; SLM) product

From the TRMM/GPM SLH V06A product, we added the unconditional variables (UnCnd) for all rain type, and modified their variable names to include conditional variables (Cnd). Please refer to the ATBD.

[Note about the missing value for conditional mean]

Note that there are two reasons for missing values for conditional mean (LHCndMean, Q1RCndMean, Q2CndMean), which can be discriminated by 'allPix' values as follows.

1. conditional mean is not defined because there is no precipitation in the grid (precipPix=0), when allPix ≠ 0.
2. missing value is given because the grid value is masked out related to the topography, when and allPix = 0.

[Note about CorrectionFactorMidlatType in SLM]

After the SLH V06B algorithm, heating (LH, Q1R, Q2) has been corrected by the CorrectionFactorMidlatType=0.88 in the area where the midlatitude algorithm is applied. In V07, because this factor is changed to be applied to only the SLM product, but not to the SLP product, the monthly mean of the L2 heating divided by the factor corresponds to the SLM product in the midlatitude area.

May 3, 2022

ATBD GPM V7: http://rain.atmos.colostate.edu/ATBD/ATBD_GPM_V7_May15_2021.pdf

Release Notes for GPROF V7 Public Release

The Goddard Profiling Algorithm is a Bayesian approach that nominally uses the GPM Combined algorithm to create its a-priori databases. Given the importance of these databases to the final product, they are worth reviewing before discussing particular changes to the algorithm. GPROF V03 was implemented at the launch of the GPM mission and thus had no databases from the GPM satellite itself. Instead, databases were made from a combination of TRMM, Cloudsat, ground based radars and models. V04 used the GPM generated databases but had a very short lead time as the radar and combined algorithm were in flux until nearly the date of the public release. Because the V04 of the Combined algorithm appeared to significantly overestimate precipitation over land, the a-priori databases were constructed from the Combined Algorithm (V04) over ocean, but the DPR Ku (V04) over land and coastal regions. The very short lead time to produce the a-priori databases led to insufficient testing of GPROF V04 that resulted in some less-than ideal retrievals.

GPROF V05 retained the previous version (i.e. V04) of the Combined and DPR-Ku products for its databases, but improved some of the ice hydrometeor simulations in order to get better agreement between computed and simulated brightness temperatures. Additional changes were made to retrievals of high latitude oceanic drizzle and snowfall over land as the DPR sensitivity of 12 dBZ (and therefore the Combined and Radar products) was shown to miss substantial amounts of drizzle and light to moderate snowfall events. Drizzle in the a-priori database was matched to the CloudSat based probability of rainfall and this was partitioned between cloud- and rain water. This increased rain water at high altitudes to agree better with CloudSat and ERA and MERRA re-analyses, but continued to be low relative to these estimates.

There is not GPROF V06. Instead, GPROF jumped to GPROF V07 to mirror the other GPM products that were produced starting in May 2022. In GPROF V07, the a-priori databases were constructed singularly from the Combined Radar/Radiometer Algorithm (V07) where it sees precipitation, while non-precipitating and light drizzle (up to 0.2 mm/hr) are created from the operations Microwave Integrated Retrieval System (MiRS) Optimal Estimation retrieval. The GPROF V07 database, as done previously, uses only the middle 21 pixels of the radar scan. This subset of the CMB product produces more rain than the entire swath, and V7 produces substantially more rain than the CMB product used in GPROF V05. Rain rates have thus increased significantly, in the 12% range globally.

Some changes were made to the coast and land surface types for GPROF V07. Previous versions of GPROF showed spurious precipitation in coastal areas. To improve estimates, the V05 coast surface class was split into three classes of decreasing ocean/water percentages: water coast, mixed coast and land coast.

Similarly, areas of complex terrain have been identified as lacking orographically enhanced precipitation, compared to ERA5 and High Resolution Rapid Refresh (HRRR) model data. A mountain rain and mountain snow class are included in GPROF V07. For the mountain rain class, the surface type was further subclassified with an airmass lifting index (ALI), based on whether atmospheric conditions were stratiform and orographically enhanced. The Combined product precipitation used in the a-priori database for the two new mountain classes was also scaled to match ERA5, which was considered to be a better mountain precipitation climatology.

Over land, the US based MRMS data was used to build a-priori databases for snow covered surfaces of each of the constellation's radiometers. Five years of MRMS data were matched up with individual satellite overpasses, compared to two years in GPROF V05. While MRMS data removed much of the low bias that GPROF V04 had over snow covered surfaces, further adjustments were made to make the MRMS data spatially consistent with SNOW Data Assimilation System (SNODAS) precipitation estimates.

Sea ice a-priori databases in GPROF V07 are created with ERA5 precipitation, since the DPR is insufficient over these surface types. As with the MRMS data, the sea ice database was only 2D and did not contain the vertical hydrometeor profiles, so no profile information is available from the GPROF retrieval over sea ice covered surfaces.

A change has been made to the GPROF V05 profile species, which were: rain water content, cloud water content, ice water content, snow water content and graupel/hail content. In GPROF V07, the profile species are: rain water content, cloud water content, snow water content, graupel/hail content and latent heating. However, the graupel/hail content and latent heating profiles are currently set to missing, with the latter to be implemented in the next version.

A final modification made to GPROF is the determination of a precipitation threshold. GPROF V04 reported an unconditional rain rate and a probability of precipitation, it was up to the user to set a threshold (either in probability or rain rate) if rain/no rain information was needed. While GPROF V05 reported the same information, the algorithm internally decided if the pixel was precipitating or not, and non-precipitating pixels were set to zero rainfall. This required the algorithm to replace the missing rain by slightly increasing the precipitation in the pixels that were deemed raining. GPROF V07 reverts back to the unconditional rain rate and probability of precipitation being reported, as it is really not possible for passive microwaves to distinguish clouds from very light rain in an unambiguous manner. To accommodate users who need a binary yes/no answer, a new precipitation flag has been added to the output. If the algorithm determined the pixel was most likely precipitating, the 'precipitationYesNoFlag' is set to raining.

Limited validation of GPROF V07 for GMI shows better correlations and smaller biases than GPROF V05. Statistics were run over the Continental United States with MRMS data and globally with Combined data. Even more limited validation has been done on snow due to the difficulty in getting reliable ground-based measurements.

GPROF V07 chose to wait for the latest iteration of the GPM CMB product in order better to synchronize the products. The short lead time to produce the a-priori databases, unfortunately, also led to less than full testing of GPROF V07. Little validation has been done on the constellation radiometers beyond limited comparisons with GMI (or TMI for earlier sensors) to ensure that the retrieval is performing as expected.

The GPROF V07 output file 'airmassLiftIndex' has replaced the V05 parameter labeled 'CAPE' (set to missing in GPROF V05), as it is not used.

Sims, E.M. and G. Liu, 2015: [A Parameterization of the Probability of Snow–Rain Transition](#). *J. Hydrometeor.*, **16**, 1466–1477, doi: 10.1175/JHM-D-14-0211.1.

National Operational Hydrologic Remote Sensing Center. 2004. *Snow Data Assimilation System (SNODAS) Data Products at NSIDC, Version 1*. Boulder, Colorado USA. NSIDC: National Snow and Ice Data Center. doi: <https://doi.org/10.7265/N5TB14TC>.

April 12, 2022

Caveats for the COmbined Radar-Radiometer Algorithm (CORRA) Level 2 Products in the GPM/TRMM V07 Public Releases

The GPM COmbined Radar-Radiometer Algorithm (CORRA) L2 V07 product includes precipitation estimates over the full, 245 km Ku radar swath (Ku+GMI inputs, as well as Ku+Ka+GMI inputs after May 21, 2018), and estimates over the narrower, 125 km inner swath (Ku+Ka+GMI inputs before May 21, 2018). The inputs for the GPM CORRA L2 algorithm are derived from DPR L2 and GMI L1C products. In particular, the CORRA L2 algorithm draws upon inputs from the DPR L2 Preparation Module, Classification Module, Surface Reference Technique Module, and the Vertical Structure Module. From GMI L1C, the GPM L2 algorithm inputs the intercalibrated brightness temperature observations. CORRA has also been extended to produce TRMM precipitation products from a combination of precipitation radar (PR) and TRMM microwave imager (TMI) data, using essentially the same estimation method that is applied to GPM. In this case, estimates based on only the Ku+TMI inputs over the Ku radar swath are produced, since no Ka band radar data are available from TRMM.

During the early GPM mission (prior to June 2014) many tests and modifications of the DPR performance were carried out, and these had an impact on not only DPR products but also the GPM CORRA L2 estimates that depend on them. Therefore, GPM CORRA L2 precipitation estimates from the early mission should be used with caution. A listing of the orbits impacted by these tests and modifications can be obtained from the GPM Radar Team.

Mainlobe and sidelobe clutter contamination of DPR reflectivities is reduced using radar beam reshaping and statistical corrections. The combination of these applications reduces clutter successfully over most surfaces, but there are still “exceptional” regions where clutter signatures are still evident. Also, ice-covered land surfaces produce Ku-band radar surface cross-sections at nadir view that sometime exceed the upper limit of the radar receiver range. Estimates of Ku-band path-integrated attenuation from the Surface Reference Technique Module are possibly biased in these regions. Since radar reflectivities and path-integrated attenuations are utilized by the CORRA L2 algorithm, precipitation estimates in these “exceptional” regions should be used with caution.

The current GPM CORRA L2 algorithm uses the Ku-band radar reflectivities from the Preparation Module to detect either liquid- or ice-phase precipitation. The lowest detectable reflectivity for DPR at Ku band is ~13 dBZ, and so light snow or very light rainfall may not be detected and quantified by the algorithm. The TRMM PR radar has a minimum detectable signal of ~18 dBZ, and so even more light snow and rainfall

may not be quantified by TRMM CORRA.

In addition to the impact of input data from DPR L2, there are uncertainties due to the current limitations of the CORRA L2 algorithm's physical models and other assumptions that can also have an impact on precipitation estimates. In particular, the physical models for scattering by ice-phase precipitation particles now feature realistic nonspherical particle geometries, but these particle models are still undergoing development. The scattering models for ice- and mixed-phase precipitation will likely be improved in future product releases. Also, the effects of radar footprint non-uniform beamfilling and multiple scattering of transmitted power are addressed in CORRA L2, but the strategies that have been implemented to handle these effects are not yet generalized and have not been analyzed in detail. Multiple scattering primarily affects Ka-band reflectivities, and it sometimes eliminates Earth surface reflection in regions of strong radar attenuation (although attenuation can sometimes eliminate the surface signal even if multiple scattering effects are small). Footprint non-uniform beamfilling impacts the interpretation of both Ku- and Ka-band radar data. As a consequence, CORRA L2 precipitation estimates associated with intense convection, in particular, will have greater uncertainties. Finally, the assumed *a priori* statistics of precipitation particle size distributions can have an influence on estimated precipitation. As particle size distribution data are collected during the mission, more appropriate assumptions regarding the *a priori* statistics of particle sizes will be specified in the algorithm. At this stage of the mission, however, relatively simple assumptions regarding particle size distributions have been introduced into the algorithm, and so biases in estimated precipitation rates and the associated particle size distributions can occur. The correct diagnosis of particle sizes in CORRA L2 estimates may require more general constraints on particle size distribution parameters, and these constraints are the subject of ongoing studies.

It should also be noted that both precipitation estimates and retrievals of environmental parameters from CORRA L2 have not yet been comprehensively validated using ground observations. Such a validation effort is under way and will continue to expand after the GPM/TRMM V07 release of products. Therefore, it is very important that users of these public release products keep in contact with the Combined Algorithm Team for updates on the validation of precipitation estimates and any reprocessing's of CORRA L2 products.

Preliminary validation of the GPM CORRA L2 V07 product has revealed good consistency between estimated surface precipitation rate and raingauge-calibrated radar. At footprint scale, matches of the GPM CORRA V07 with raingauge-calibrated radar (Multi-Radar Multi-Sensor [MRMS] product) over the continental US/lower Canada and coastal waters during the June - December 2018 period (post HS scan shift) yielded total low biases of 9% for the Ku+Ka+GMI product and 5% for the Ku+GMI product, with correlations to MRMS of about 0.76 for both products. Considering that the lack of DPR sensitivity contributes a low bias of approximately 7% to the total bias, these are respectable results.

Zonal mean precipitation rates agree well with zonal mean precipitation rates from the Global Precipitation Climatology Project (GPCP V3.2) product within the 40°S to 40°N latitude band over ocean backgrounds. Estimated zonal means at higher latitudes are underestimated relative to GPCP, due in part to the limited sensitivity of the DPR radar to light snow and drizzle. Over the October 2018 – December 2019 period, in the 40°S and 40°N latitude band, CORRA Ku+Ka+GMI L2 estimates over ocean are low-biased by 4% relative to GPCP, while Ku+GMI estimates over ocean are low-biased by 1%. For the same time period and latitude band, Ku+Ka+GMI and Ku+GMI CORRA L2 estimates over land are currently low biased by 13% and 9%, respectively, with the greatest biases occurring in warm, moist tropical and subtropical regimes.

Note that relative to V06, V07 CORRA Ku+Ka+GMI estimates in the 40°S and 40°N band have decreased by 2% over ocean, while Ku+GMI estimates have increased by 7%. Over land in the same latitudinal band, both Ku+Ka+GMI and Ku+GMI estimates have increased by 9% relative to V06. These changes are effected by nudging initial guess drop-size parameters closer to values established from climatological relationships, which leads to greater proportions of smaller drops and higher rain rates at the lighter end of the estimated rain spectrum, particularly over land regions, where radar-derived, path-integrated attenuations and microwave brightness temperatures do not supply additional drop-size information with great certainty. The changes are justified by the greater fidelity of mean CORRA estimates with raingauge-calibrated ground radar estimates over the continental US, better agreement of CORRA with GPCP V3.2 overall, and greater consistency of drop-size distribution parameter relationships relative to climatology.

The TRMM CORRA V07 algorithm precipitation rate estimates compare well with the GPM CORRA V07. Based upon a limited sample of crossover data derived from the April – September, 2014 GPM-TRMM overlap period, there is an overall high bias of TRMM estimates relative to GPM of approximately 6% based upon matched GPM and TRMM footprints, with a correlation of 0.73 between GPM and TRMM.

Mitigation of the low biases in CORRA L2 estimates, particularly over land, is a priority of the algorithm developers and is an active area of PMM research. A radiometer-only precipitation estimation method designed to quantify precipitation rates below DPR detection limits is currently under development and will be introduced in V08 production. In addition, an experimental product for statistically estimating precipitation at the Earth's surface within the DPR ground clutter, based on retrieved values of precipitation above the clutter (near-surface estimates), have been produced and output in CORRA V07. Although preliminary, these surface estimates are substantially increased relative to near-surface estimates, particularly in ocean regions where climatologically, precipitation tends to increase from levels above the clutter toward the surface. *It should be emphasized that these surface estimates are currently experimental, and more work will be required to stabilize and refine these estimates. Users are therefore recommended to still use near-surface*

precipitation estimates until a more rigorous and meteorologically specific clutter correction method is implemented.

There could potentially be significant changes in the CORRA L2 rain rate products in the transition from GPM V07 to V08 due to modifications and improvements of the CORRA algorithm. Since the GPM and TRMM algorithms share the same software “core”, future changes in CORRA should apply to both GPM and TRMM. Again, users of the GPM/TRMM V07 public release products should keep in contact with the Combined Algorithm Team for information regarding these changes.

GPM/TRMM CORRA L2 V06 to V07 Changes

Several modifications have been made to the GPM CORRA L2 algorithm in the transition from V06 to V07. These changes can be categorized as changes in algorithm function and changes in output parameters and format. Regarding algorithm function, the basic algorithm mechanics (i.e., estimation methodology) has not changed, and the same mechanics are applied to both the GPM and TRMM data. The GPM estimation method filters ensembles of DPR Ku reflectivity-consistent precipitation profiles using the DPR Ka reflectivities, path integrated attenuations and attenuated surface radar cross-sections at Ku and Ka bands, and GMI brightness temperatures. The filtered profile ensembles are consistent with all of the observations and their uncertainties, and the mean of the filtered ensemble gives the best estimate of the precipitation profile. The TRMM CORRA algorithm filters PR Ku reflectivity-based precipitation profile estimates using path integrated attenuations and attenuated surface radar cross-sections at Ku band, as well as TMI brightness temperatures.

Probably the most impactful change in CORRA V07 concerns the way in which the precipitation drop-size distribution *a priori* assumptions are applied. In both V06 and V07, the precipitation drop-size distribution is assumed to follow a normalized gamma distribution, and the intercept, N_w , and mass-weighted mean diameter, D_m , are adjusted in CORRA during the estimation process. Initial guess values of N_w are drawn from a lognormal distribution and combined with the Ku reflectivity data to derive a D_m profile using a modified Hitschfeld-Bordan procedure. The D_m values are then used to make a second estimate of the N_w , using an empirical $\log N_w - D_m$ curve. Empirical $\log N_w - D_m$ relationships were previously established by Dolan et al. (2018), Bringi et al. (2021) and others, using disdrometer and microphysics probe observations at various locations over the globe. The initial N_w are nudged toward the empirical N_w , and the nudged values are used to again estimate a revised, initial D_m profile using Hitschfeld-Bordan. This two-step initial guess procedure moves initial N_w values higher for lower D_m (lighter precipitation) and lower for higher D_m (heavier precipitation).

In CORRA V06, the procedure just described was only applied to stratiform precipitation, and there were somewhat different drop-size distribution treatments for ocean and land regions. In CORRA V07, there is (a) no distinction between ocean and land in the initial drop-size distribution adjustment, (b) the empirical curve relating $\log N_w$ and D_m for convective precipitation is shifted to slightly higher $\log N_w$ values relative to stratiform, and (c) the nudging of the initial guess N_w toward the empirical values is done more strongly. The upshot of these changes is that the proportion of smaller drops in the initial guess generally increases for smaller D_m , and this leads to increases in precipitation rates at the lighter end of the precipitation spectrum. For heavier precipitation, drop-size distribution adjustments tend to be more controlled by path integrated attenuations and brightness temperatures, if they are reliable. Overall, however, substantial increases in estimated total precipitation are realized in the mean, especially over land regions. Biases of CORRA V07 relative

to ground validation radar and GPCP over land are reduced, and disparities of Ku+Ka+GMI estimates and Ku+GMI estimates over ocean are lessened. In addition, the ocean vs. land contrast of estimated drop-size distributions is less, and the relationships of estimated $\log N_w$ and D_m are closer to empirical relationships.

Introduced in CORRA V07 is a clutter or “blind zone” correction of near-surface (above clutter) estimates to create experimental, estimated-surface precipitation rates. The clutter zone of the DPR is roughly 0.7 km at nadir view, rising to over 2 km at the swath edges. Climatological relationships between the near-surface estimates and “surface” estimates (actually, at about 0.8 km above the Earth’s surface), were established using nadir-view CORRA V07 precipitation rate profile estimates for ocean/land and convective/stratiform classes. This work follows similar studies by Hirose and Nakamura (2004), Liu and Zipser (2013), and Hirose et al. (2021), but uses CORRA V07 profiles to establish the vertical structure climatologies. The climatological relationships are used to scale the near-surface precipitation rates to statistically estimate surface precipitation rates when the surface level is within the clutter. Over ocean, where cloud updraft speeds are relatively weak, climatological mean precipitation rate profiles tend to increase from radar bins just above the clutter toward the surface, and so precipitation rates are significantly increased over ocean (8%) relative to near-surface values. Over land, climatological profiles tend to show less variation with height, and smaller increases in surface estimates are realized (3%). *Since the climatological precipitation profiles were established based on a limited number of CORRA-retrieved profiles, this clutter correction is deemed experimental in V07, and users are recommended to still use near-surface precipitation estimates until a more rigorous and meteorologically specific clutter correction method is implemented.*

New output variable names and formats have also been introduced in CORRA V07. In particular, the structure name for the Ku+Ka+GMI estimates are called KuKaGMI, and likewise the structure name for the Ku+GMI estimates is now KuGMI. These replace the NS and MS mode structure names of V06, respectively. Similarly, the structure name for the Ku+TMI estimates is now KuTMI. Also, a new structure called OptEst has been included to hold variables derived from an optimal estimation method that fits non-precipitating variables like temperature, humidity, cloud liquid water, and surface emissivity parameters to the radiometer data. These output variables are currently just placeholders, but they will be used in the future to establish background conditions for radiometer-only estimates of precipitation in regions where radar reflectivities are below the minimum detectable of the DPR. Finally, selected variables that were previously estimated at only specified nodal bins of the radar profiles are now defined at full vertical resolution. These include the N_w and D_m profiles, their initial guesses, as well as the profiles of total hydrometeor water contents and fluxes and the liquid portions of those water contents and fluxes. These changes will make it easier to extract and interpret the profiles from CORRA V07.

References:

- Bringi, V., M. Grecu, A. Protat, M. Thurai, and C. Klepp, 2021: Measurements of rainfall rate, drop size distribution, and variability at middle and higher latitudes: application to the Combined DPR-GMI Algorithm *Remote Sens.*, **13**, 2412; <https://doi.org/10.3390/rs13122412>.
- Dolan, B., B. Fuchs, S. A. Rutledge, E. A. Barnes, and E. J. Thompson, 2018: Primary modes of global drop size distributions. *J. Atmos. Sci.*, **75**, 1453-1476.
- Hirose, M., and K. Nakamura, 2004: Spatiotemporal variation of the vertical gradient of rainfall rate observed by the TRMM Precipitation Radar. *J. Climate*, **17**, 3378-3397.
- Hirose, M., S. Shige, T. Kubota, F. A. Furuzawa, H. Minda, and H. Masunaga, 2021: Refinement of surface precipitation estimates for the Dual-frequency Precipitation Radar on the GPM Core observatory. *J. Met. Soc. Japan* (early online release) DOI:10.2151/jmsj.2021-060.
- Liu, C., and E. J. Zipser, 2013: Why does radar reflectivity tend to increase downward toward the ocean surface, but decrease downward toward the land surface? *J. Geophys. Res.: Atmos.*, **118**, 135-148, doi:10.1029/2012JD018134, 2013.